

NWRI CONTRIBUTION 88-75

**STAGE-DISCHARGE EQUATIONS FOR
SHARP CRESTED COMPOSITE WEIRS**

by

Peter Engel and D. Doede

Research and Applications Branch
National Water Research Institute
Canada Centre for Inland Waters
867 Lakeshore Road, P.O. Box 5050
Burlington, Ontario, Canada L7R 4A6

April 1988

MANAGEMENT PERSPECTIVE

Comparison of laboratory data and theory shows that in situ calibrations of composite weirs are required to establish stage-discharge relations. Modifications to existing weirs should be undertaken with caution.

Dr. J. Lawrence
Director
Research and Applications Branch

PERSPECTIVE DE GESTION

La comparaison des données de laboratoire et de la théorie montre qu'il est nécessaire d'étalonner in situ les déversoirs composites pour établir les courbes des débits jaugés. Toute modification apportée aux déversoirs existants doit donc l'être avec prudence.

Dr. J. Lawrence

Directeur

Direction de la recherche et des applications

SUMMARY

The Water Survey of Canada uses compound weirs at some of their hydrometric stations. A theoretical and experimental study was conducted to investigate the behaviour of such weirs near the crest transition. The results show that, while theoretical methods describe the stage-discharge equations very well, on-site calibrations should be conducted to obtain the necessary accuracy. Analysis also indicates that careful consideration must be given to the geometric proportioning of the weir cross-section.

RÉSUMÉ

La division des relevés hydrologiques du Canada se sert de déversoirs composites dans certaines de ses stations hydrométriques. Une étude théorique et expérimentale a été effectuée afin d'évaluer le fonctionnement de ces déversoirs près de la transition de crête. Les résultats obtenus montrent que, bien que les méthodes théoriques décrivent très bien les équations de débit jaugé, il faut quand même procéder à des étalonnages sur place pour obtenir l'exactitude nécessaire. L'analyse indique également qu'il faut bien tenir compte du dimensionnement géométrique de la section du déversoir.

TABLE OF CONTENTS

	<u>Page</u>
MANAGEMENT PERSPECTIVE	i
SUMMARY	ii
1.0 INTRODUCTION	1
2.0 STAGE DISCHARGE EQUATIONS	1
2.1 Equations Developed by Water Survey of Canada	1
2.2 Equations from First Principles	2
2.3 Discharge Coefficients and Effects of Fluid Properties.	4
2.3.1 The v-notch weir component	4
2.3.2 The rectangular weir component	6
3.0 EXPERIMENTAL SET-UP AND PROCEDURE	7
3.1 Description of the Flume	7
3.2 Measurement of Discharge	8
3.3 Measurement of Water Levels	8
3.4 The Compound Weir	9
3.5 Test Procedure	9
4.0 RESULTS	9
4.1 Plot of Experimental Data	9
4.2 Plot of Theoretical Equations	10
4.3 Effect of Weir Proportions	10
5.0 CONCLUSIONS	12

REFERENCES

TABLES

FIGURES

1.0 INTRODUCTION

The Water Survey of Canada has hydrometric stations at five streams flowing into Perch Lake. Because the streams are very small, 90° V-notch weirs are used to measure the discharges. On some occasions these weirs have been overtopped. In order to obtain reliable records for the high flow events, the original weirs have been modified by adding a rectangular cross-section to the top resulting in a compound weir as shown schematically in Figure 1. To extend the existing stage-discharge curves, theoretical equations were developed. These equations were reviewed by Engel (1986) and found to be theoretically correct. However, the theoretical equations may not completely reflect the effect of the transition in the crest from V-notch to rectangular weir. It was therefore recommended by Engel (1986) that a hydraulic model study be conducted to determine the error, if any, incurred in discharge determination due to this effect. Such effects will be particularly important if the water surface is close to the transition for significant lengths of time.

This report presents the results of a brief theoretical and experimental investigation conducted at the Hydraulics Laboratory of the National Water Research Institute. The work is in support of the Water Survey of Canada (WSC) at Guelph, Ontario.

2.0 STAGE-DISCHARGE EQUATIONS

2.1 Equations Developed by Water Survey of Canada

The general form of the rating equation prepared by WSC is given as

$$Q = C_1 H^n \quad H \leq a \quad (1)$$

$$Q = C_1 H^n - C_1 (H-a)^n + C_2 L (H-a)^{1.5} \quad H > a \quad (2)$$

in which Q = discharge, C_1 and C_2 are coefficients, H = the head with respect to the apex of the V-notch, a = depth of the V-notch, L = the total length of the added horizontal crest of the weir extension. The variables are shown schematically in Figure 1.

Equation (2) is determined by means of superposition of discharges obtained by using the standard V-notch equation and rectangular weir equation, both for the case of sharp crests. This method is theoretically correct as long as all the component parts have a free surface (Bos, 1976). The principle of superposition with reference to Figure 2, is applied as follows by taking

$$Q = Q_A - Q_B + Q_C \quad (3)$$

where $Q_A = C_1 H^n$ = discharge due to the V-notch as if it applied over the full head H , $Q_B = C_1 (H - a)^n$ = the discharge passing through the shaded areas in Figure 2, which in effect is equivalent to a V-notch with a head of $(H - a)$. This discharge Q_B must be subtracted to avoid double counting. $Q_C = C_2 L (H - a)^{1.5}$ = the discharge for each of the rectangular sections having a length of $L/2$ for a total horizontal crest of length L .

2.2 Equation from First Principles

The total discharge at a given head H , with reference to Figure 3 can be expressed in the integral form for $H \leq a$ as

$$Q = 2\sqrt{2g} C_\phi \tan \frac{\phi}{2} \int_0^a y (H - y)^{1/2} dy \quad (4)$$

and for $H \geq a$

$$Q = 2\sqrt{2g} C_{\phi} \tan \frac{\phi}{2} \left[\int_0^a y(H - y)^{1/2} dy + a \int_a^H (H - y)^{1/2} dy \right] + 4\sqrt{2g} C_R \ell \int_a^H (H - y)^{1/2} dy \quad (5)$$

where g = acceleration due to gravity, ϕ = angle at the apex of the V-notch, y = variable distance above the apex of the V-notch, a = the height of the V-notch weir, ℓ = the length of the horizontal crest extension, d denotes a derivative of the indicated variable, C_{ϕ} and C_R are discharge coefficients for the V-notch and rectangular weir extension crests respectively. Integration and simplification results in

$$Q = \frac{8\sqrt{2g}}{15} C_{\phi} \tan \frac{\phi}{2} H^{5/2} \quad \text{for } H \leq a \quad (6)$$

and

$$Q = \frac{8\sqrt{2g}}{15} C_{\phi} \tan \frac{\phi}{2} \left[H^{5/2} - (H - a)^{5/2} \right] + \frac{4\sqrt{2g}}{g} C_R \ell (H - a)^{3/2} \quad \text{for } H > a \quad (7)$$

After noting that ℓ in equation (7) is equal to $L/2$ in equation (2) one obtains

$$Q = \frac{8\sqrt{2g}}{15} C_{\phi} \tan \frac{\phi}{2} \left[H^{5/2} - (H - a)^{5/2} \right] \\ + \frac{2\sqrt{2g}}{3} C_R L (H - a)^{3/2} \quad \text{for } H > a \quad (8)$$

Comparison of equations (1) and (6) shows that

$$C_1 = \frac{8\sqrt{2g}}{15} \tan \frac{\phi}{2} C_{\phi} \quad (9)$$

while from equations (2) and (8) one obtains

$$C_2 = \frac{2\sqrt{2g}}{3} C_R \quad (10)$$

In addition it is quite evident that the exponent n in equation (1) and (2) should have the value of $5/2$. Therefore, equation (1) and (2) are valid as long as the values of C_1 and C_2 are in accordance with equations (9) and (10). Values of C_{ϕ} and C_R are determined from experiments.

2.3 Discharge Coefficients and Effects of Fluid Properties

The stage discharge equations for the compound weir consist of a V-notch component and a rectangular weir component.

2.3.1 The V-notch component

The coefficient of discharge is a function of fluid properties, crest geometry, head H , weir dimensions, and roughness of upstream face of the weir. This can be expressed by writing

$$C_{\phi} = C_{\phi} [\rho, \mu, \sigma, H, P, B, \phi, g, K_w] \quad (11)$$

where: ρ = density of the fluid, μ = dynamic viscosity of the fluid, σ = surface tension of the fluid, H = head, P = distance from V-notch apex to the base of weir on upstream side, B = width of approach channel, ϕ = angle of apex of V-notch, g = acceleration due to gravity, K_w represents the roughness of the upstream face of the weir wall.

Using dimensional analysis one obtains

$$C_{\phi} = C_{\phi} \left[\frac{\rho g^{1/2} H^{3/2}}{\mu}, \frac{\sigma}{\rho g H^2}, \frac{H}{P}, \frac{P}{B}, \phi, K_w \right] \quad (12)$$

For the flow encountered $\rho g^{1/2} H^{3/2} / \mu$ and $\sigma / \rho g H^2$ should not be important except for the low flows (i.e., $H < 3$ cm). For heads higher than that, the fluid properties effect decreases as the head increases. To avoid the fluid properties problem Kindsvater and Carter (1957) have recommended an effective head given by

$$H_e = H + K_H \quad (13)$$

where H_e = the effective head, H = measured head and K_H represents the combined effects of the fluid properties represented by the terms $\rho g^{1/2} H^{3/2} / \mu$ and $\sigma / \rho g H^2$ in Equation (12). For a sharp-crested weir, K_H itself varies with the angle ϕ and this is shown in Figure 4. The roughness factor K_w is used here to take into account the effects of increasing the roughness of the upstream face of the weir wall. If algae growth occurs or some other factors are allowed to increase the surface roughness, then the vertical velocity component of the nappe at the face, will decrease, causing an increase in the horizontal component resulting in an increase in the discharge coefficient C_{ϕ} . If the upstream face is kept in a constant

condition, then the effects of K_w can be omitted. Therefore, Equation (12) is now reduced to

$$C_\phi = C_\phi \left[\frac{H}{P}, \frac{P}{B}, \phi \right] \quad (14)$$

If $H/P < 0.4$ and $P/B < 0.2$, the V-notch weir is fully contracted and C_ϕ is a function of only the notch angle ϕ as shown in Figure (5) (Bos, 1976). If, however, the contraction of the nappe is not fully developed, that is, if $H/P > 0.4$ and $P/B < 0.2$, then the discharge coefficient C_ϕ can be read from Figure (6).

2.3.2 The rectangular weir component

The coefficient of discharge for the rectangular weir is also a function of fluid properties, crest geometry, head H , weir dimensions and texture of the upstream face of the weir wall.

This can be expressed by writing

$$C_R = C_R \left[\rho, \mu, \sigma, H, P, b, B, g, k_r \right] \quad (15)$$

where: b = the width of the weir, B = width of approach channel and all other terms have been previously defined. Using dimensional analysis one obtains

$$C_R = C_R \left[\frac{\rho g^{1/2} H^{3/2}}{\mu}, \frac{\sigma}{\rho g H^2}, \frac{H}{P}, \frac{b}{B}, k_r \right] \quad (16)$$

Once again, the terms $\rho g^{1/2} H^{3/2} / \mu$, $\sigma / \rho g H^2$ account for the fluid properties which are most significant at the low heads. These properties are accounted for (Kindsvater, Carter, 1957) by using an effective head H_e according to Equation (13) and an effective width b_e which is given by

$$b_e = b + K_b \quad (17)$$

A constant value of $K_H = 0.001$ m is recommended for all values of the ratios H/P and b/B to obtain H_e (Bos 1976). Empirically, defined values for K_b as a function of the ratio b/B are given in Figure 7, which shows considerable variability in the range $.5 < b/B < 2.0$. The wall surface texture, as in the case of the V-notch weir, will result in an increase in C_R if the surface roughness increases. Assuming, a smooth surface texture, and having accounted for the fluid properties, through Equation (13) and (17), then the coefficient of discharge becomes

$$C_R = C_R \left[\frac{H}{P}, \frac{b}{B} \right] \quad (18)$$

The variation of C_R with H/P and b/B is given in Figure 8 as C_R vs H/P with b/B as a parameter. The curves show that there can be a significant effect of both H/P and b/B .

3.0 EXPERIMENTAL SET-UP AND PROCEDURE

3.1 Description of the Flume

The experiments were conducted in a glass walled flume, rectangular in cross-section, having the following dimensions:

Width	2.0 m
Length	21.5 m
Height of Walls	0.75 m

Water is supplied to the flume from a large constant head tank which is fed by three axial flow pumps with a combined maximum output of about $0.8 \text{ m}^3/\text{s}$. From the constant head tank the water passes through a 16 in (0.4 m) diameter pipe which is terminated by a diffuser in the

head box of the flume. Baffles and screens are placed in the head box to further ensure a satisfactory velocity distribution over the cross-section of the flow at the entrance to the rectangular flume channel. The depth of the flume can be controlled by vertical adjustable louvres.

3.2 Measurement of Discharge

Discharge measurements were made using a large calibrated volumetric tank. The overflow from the constant head tank was diverted into the volumetric tank where it was measured to an accuracy of better than $\pm 1\%$. Once the overflow was measured the discharge in the flume could simply be determined from the relationship

$$Q_f = Q_p - Q_o \quad (19)$$

where Q_f is the discharge in the flume in m^3/s , Q_p is the discharge from the pre-calibrated pumps entering the constant head tank in m^3/s and Q_o is the overflow in m^3/s .

3.3 Measurement of Water Levels

All water levels were measured using stilling wells fabricated from a 5 cm diameter acrylic cylinder fitted with Mitutoyo point gauges mounted on top as shown in Figure 9. The point gauges have a resolution of 0.05 mm. The intake for this stilling well was placed sufficiently upstream of the crest to ensure that the draw down of the nappe did not affect the water level measurements. The zero of the gauge was set to coincide with the elevation of the apex of the V-notch of the compound weir.

3.4 The Compound Weir

The test weir was built out of 3/4" plywood and placed in the 2 metre flume as shown in Figure 10. All surfaces were treated with wood preservatives, all joints were carefully sealed and no significant leakage was noted at any time during the tests. The weir plate was fabricated from sheet aluminum having a thickness of 1/16" (1.6 mm) with a square machined edge at the crest. The dimensions of the composite weir are given in Figure 11.

3.5 Test Procedure

The discharge over the weir was set at a particular value and the water level in the stilling well allowed to come to an equilibrium position after which the gauge height was read and the head above the weir crest computed. Pairs of discharge and head were obtained over the full operating range of the weir. In all cases the tail water was allowed to flow unobstructed to ensure that there was no weir submergence at any time. The behaviour of the compound weir for different flows can be seen in Figure 12. The experimental data are given in Table 1.

4.0 RESULTS

4.1 Plot of Experimental Data

The data in Table 1 were plotted in Figure 13 as Q vs H on logarithmic coordinates. For flows in the V-notch, that is for $H \leq 15$ cm, the plot shows a curve of constant slope as Q increases with H up to the value of $H = 15$ cm, the point of transition. Above the transition of the weir, the plot exhibits a sudden increase in discharge for a small increase in head, with the rate of increase declining as the head becomes large. This behaviour is the consequence of the change in geometry from the V-notch to the longer

cross-section added to the flow by the horizontal weir extensions. As the head increases, the proportion of the discharge contributed through the V-notch becomes relatively smaller and one should expect that in the limit as H becomes large enough, the curve should approach the slope characteristic of a rectangular weir.

4.2 Plot of Theoretical Equations

Using equations (6) and (8) together with the discharge coefficients and effective head adjustments from Figures 5, 6, 7 and 8, the discharge was computed over the range of head H given in Figure 13. The results were plotted for comparison with the measured data in Figure 13. The results show that the theoretical equation tends to underestimate the discharge, indicating that the adjustment in the discharge coefficient and the compensation for fluid properties do not fully account for all the processes governing the flow over the test weir. Nevertheless, the theoretical curve reveals the trend of the measured stage-discharge data very well, especially in the vicinity of the transition.

The fact that the theoretical curve tends to underestimate may be due to several factors which are site specific. Such effects cannot be clearly defined and therefore each weir should be calibrated in place. Physical measurements together with the theoretical equations should result in a reliable stage-discharge relationship.

4.3 Effect of Weir Proportions

The sudden increase in slope of the stage-discharge curve at the transition, shown in Figure 13, is due to the sudden increase in the weir cross-section provided by the rectangular weir extension. For a given notch angle ϕ , the degree to which the weir transition affects the slope of the stage-discharge curve, must depend on the ratio ℓ/a . ($\ell = L/2$ in Figure 3).

Equation (8) was solved for the case of $\phi = 90^\circ$ and several cases of ℓ/a , over the same range of head as given in Figure 13. The results are plotted in Figure 14. The family of curves shows how the effect of the transition becomes more significant as ℓ/a increases from 0 to 3.0. The implication of this is that the weir becomes less reliable near the transition as ℓ/a becomes larger. In other words, a small error in measuring the head will result in a large error in determining the discharge. This error increases as ℓ/a increases. Therefore, if a compound weir, consisting of a 90° V-notch weir with rectangular weir extension is used, then one should strive for a combination of ℓ and a , which makes ℓ/a as small as possible.

5.0 CONCLUSIONS

5.1 Theoretical analysis shows that the equations proposed by Water Survey of Canada are correct. The coefficients C_1 and C_2 given in these equations should be obtained from direct calibration for each weir. The values of the coefficients should correspond closely with the values

$$C_1 = \frac{8\sqrt{2g}}{15} C_\phi \tan \frac{\phi}{2}$$

and

$$C_2 = \frac{2\sqrt{2g}}{3} C_R$$

5.2 The theoretical curve predicts the stage discharge curve very well. The use of equations (7) and (8) and (1) and (2) together with direct measurements of head and discharge, will provide reliable calibrations for compound weirs of the type considered here.

- 5.3 Compound weirs should be designed so that the ratio z/a is as small as possible. This will minimize the error in determining the discharge as a result of small errors in measuring the head.

REFERENCES

- Bos, M.G. 1976. Discharge Measurement Structures. Delft Hydraulics Laboratory publication No. 161, Delft, the Netherlands.
- Engel, P. 1986. Stage Discharge Ratings for Perch Lake Hydrometric Stations. Hydraulics Division Technical Note Report No. 87-08. National Water Research Institute, Burlington, Ontario, Canada.
- Kindsvater, C.F., R.W.C. Carter, 1957. Discharge Characteristics of Rectangular Thin-Plated Weirs. Journal of Hydraulics Division, ASCE, Vol. 83, No. HY6, Paper No. 1453.

TABLE 1
Experimental Data

Test No.	Head cm	Discharge l/s
1	5.28	1.10
2	6.79	1.90
3	7.63	2.50
4	9.30	4.0
5	10.49	5.5
6	11.54	6.9
7	13.53	9.5
8	13.85	10.2
9	14.27	10.9
10	14.89	12.4
11	15.34	14.1
12	15.64	15.9
13	16.09	18.3
14	16.38	19.3
15	16.81	23.5
16	17.19	25.8
17	18.21	33.8
18	19.91	47.2
19	22.14	72.0
20	24.27	99.3
21	26.13	123.5
22	28.27	153.5
23	30.28	183.1
24	32.98	227.8

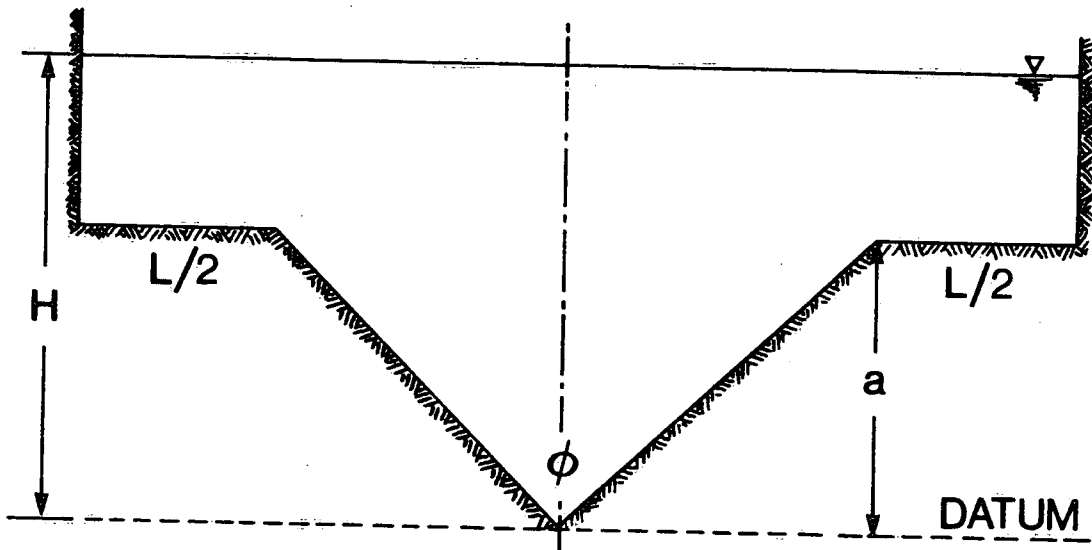


FIGURE 1. GENERAL CROSS-SECTION OF WEIR

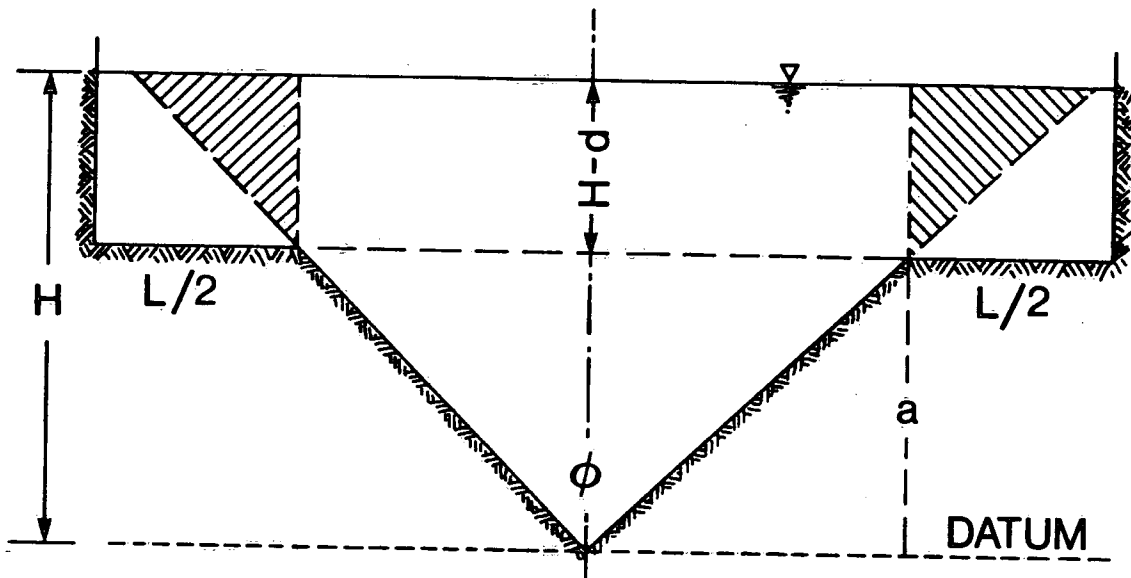


FIGURE 2. SUPER-POSITION OF WEIR SECTIONS

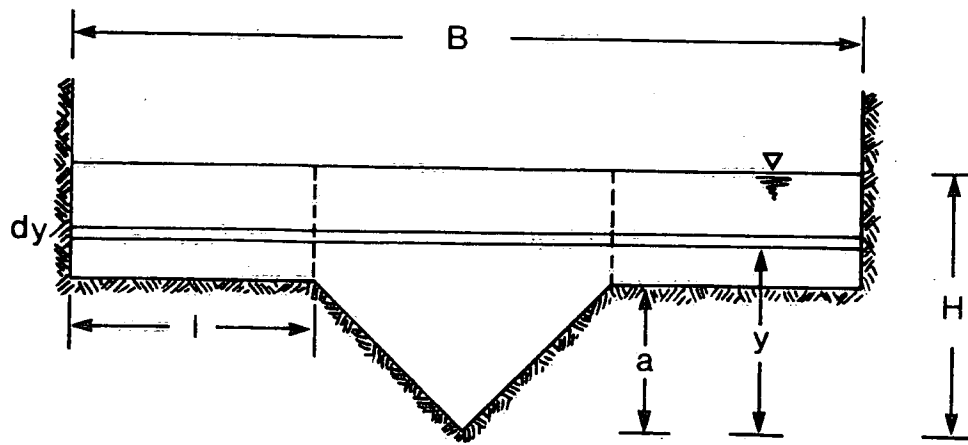


FIGURE 3. DEFINITION DIAGRAM FOR THEORETICAL EQUATIONS

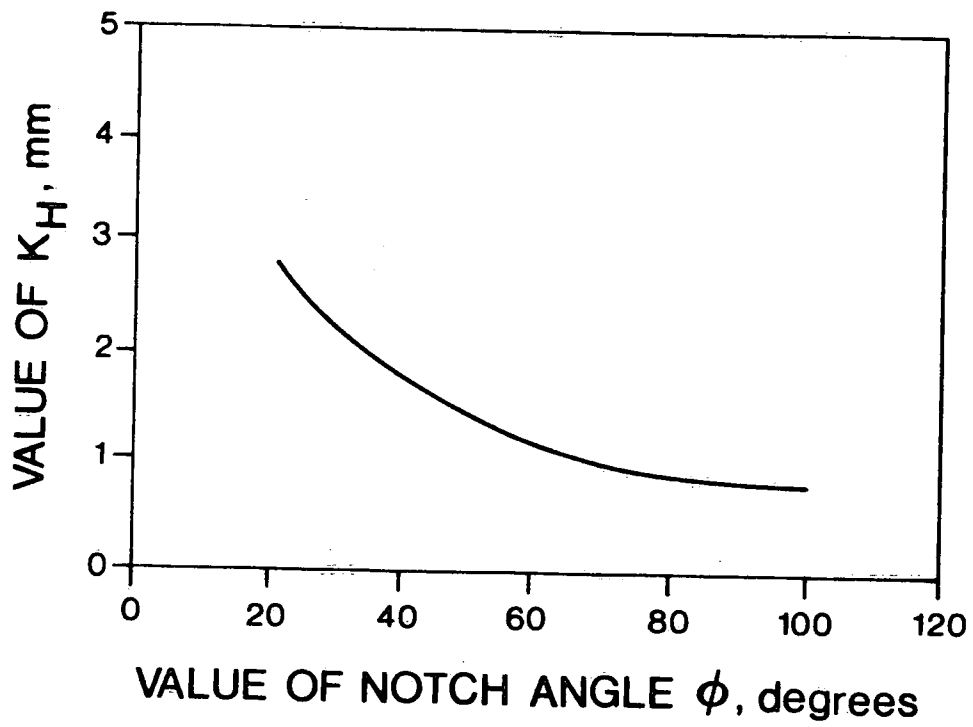


FIGURE 4. K_H AS A FUNCTION OF ϕ

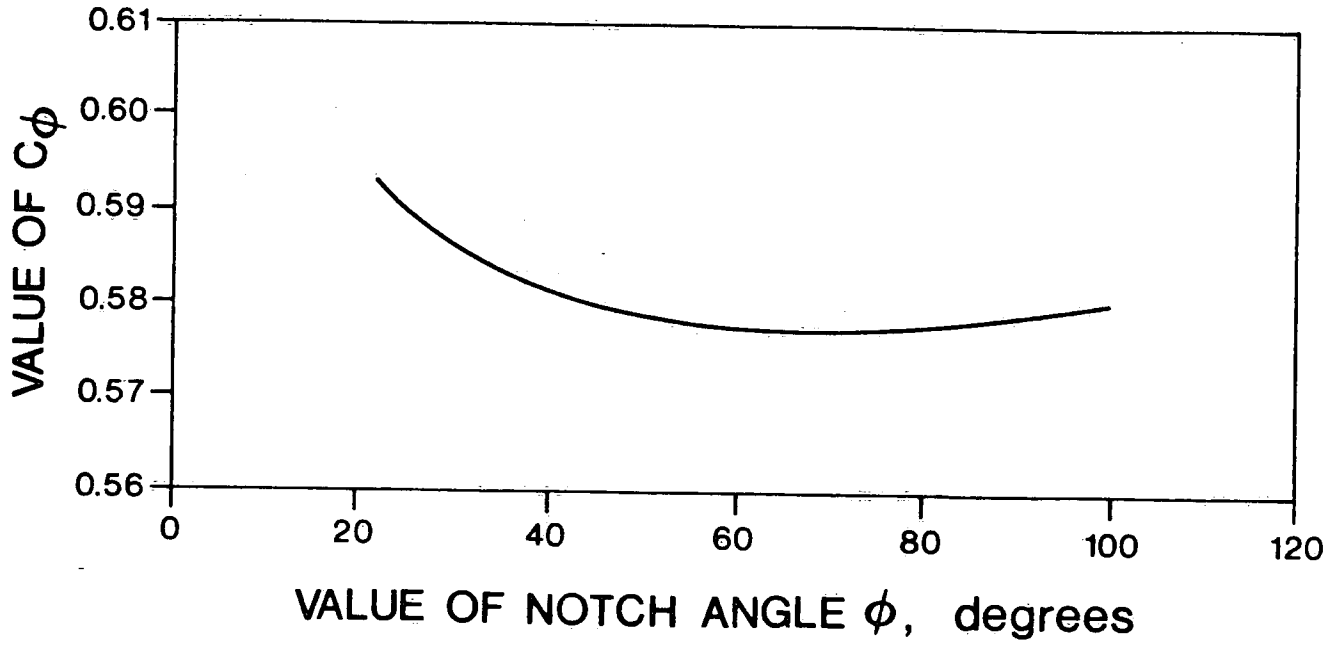


FIGURE 5. C_ϕ AS A FUNCTION OF ϕ FOR FULLY CONTRACTED WEIR

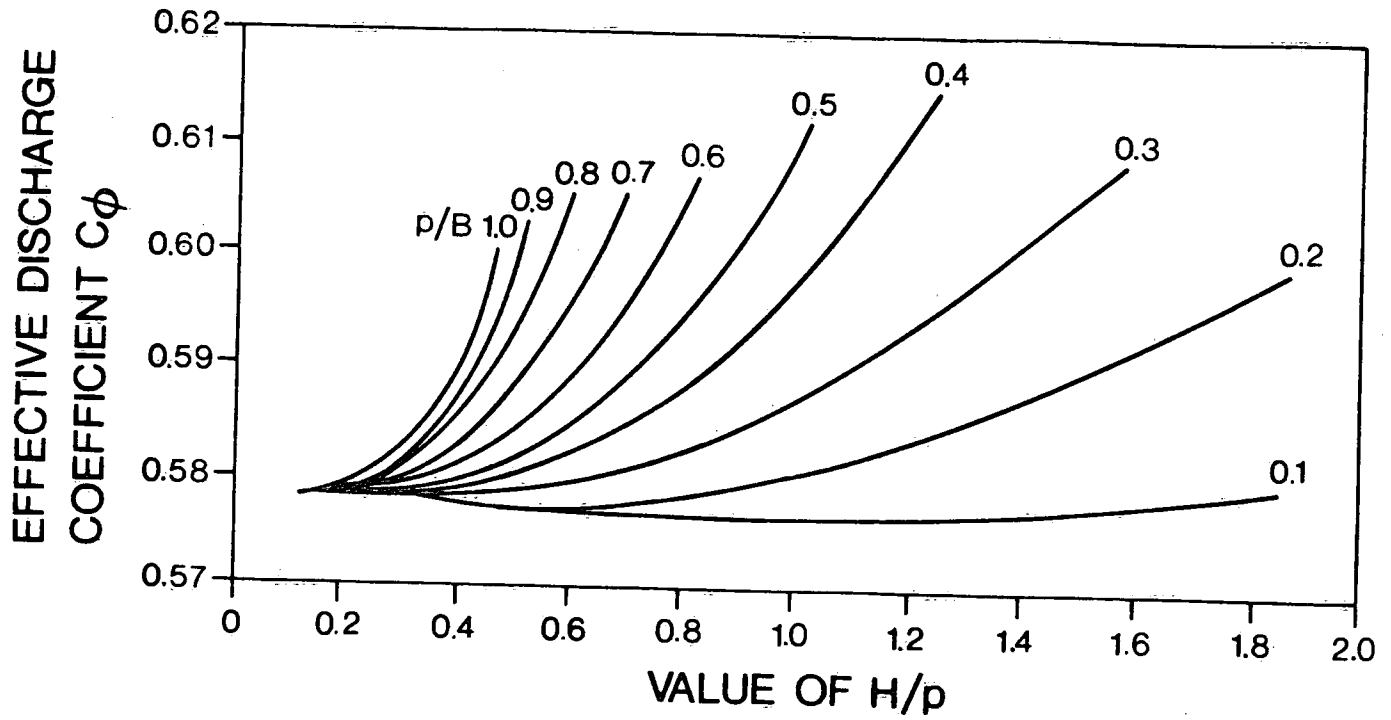


FIGURE 6. C_ϕ AS A FUNCTION OF H/P & P/B

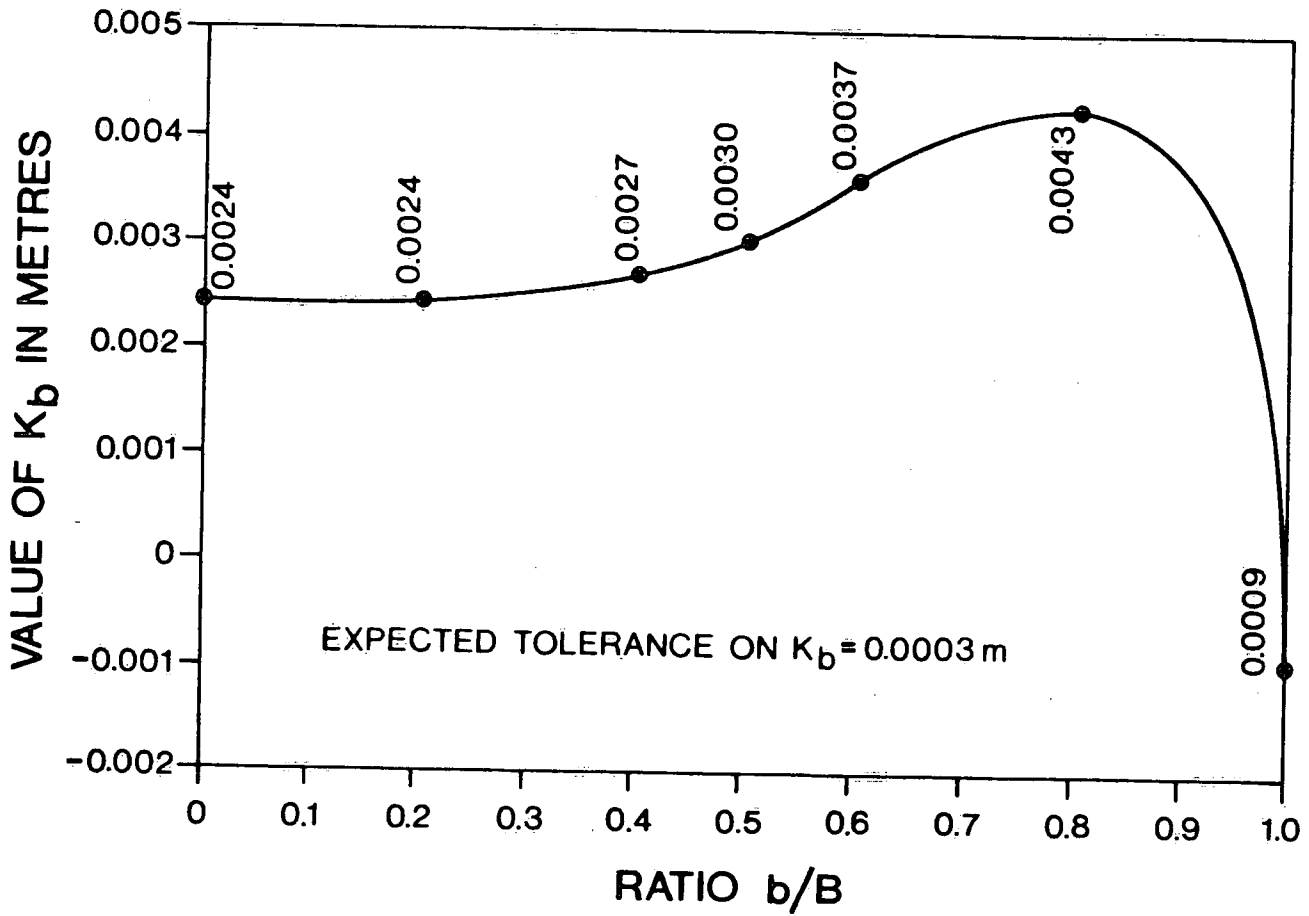


FIGURE 7. K_b AS A FUNCTION OF b/B

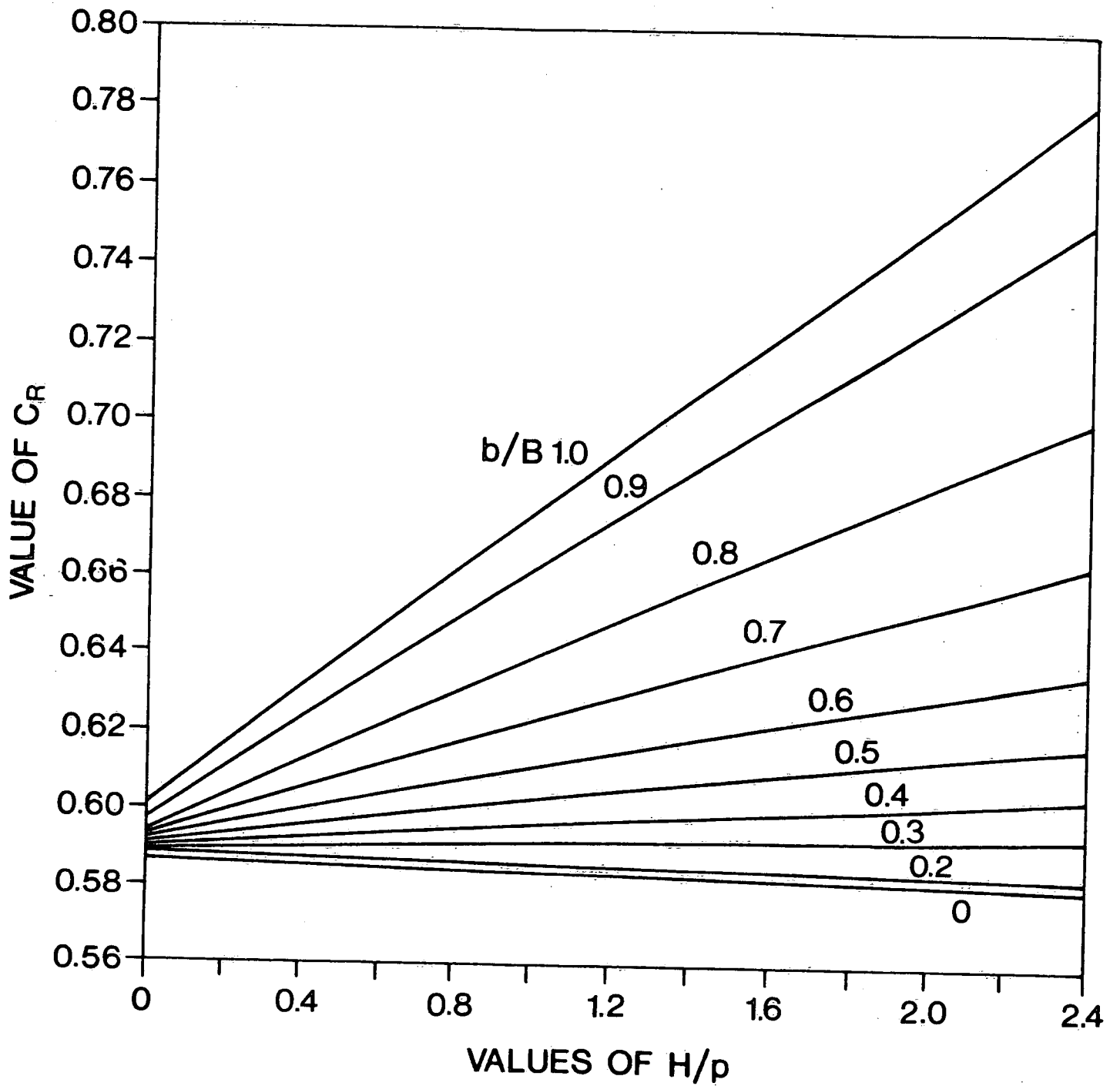


FIGURE 8. C_R AS A FUNCTION OF H/P & b/B

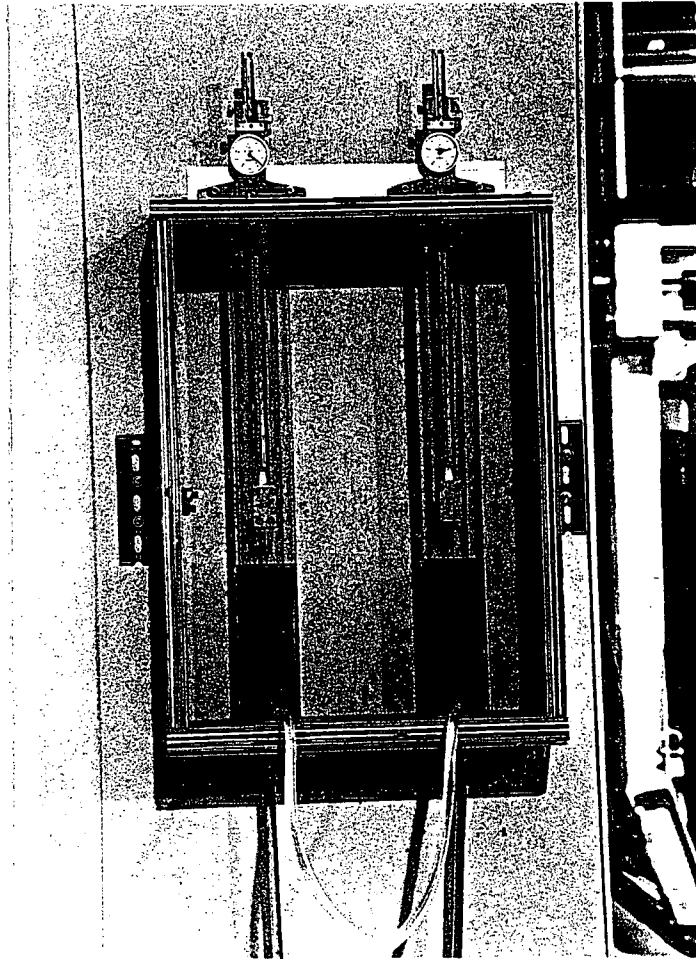
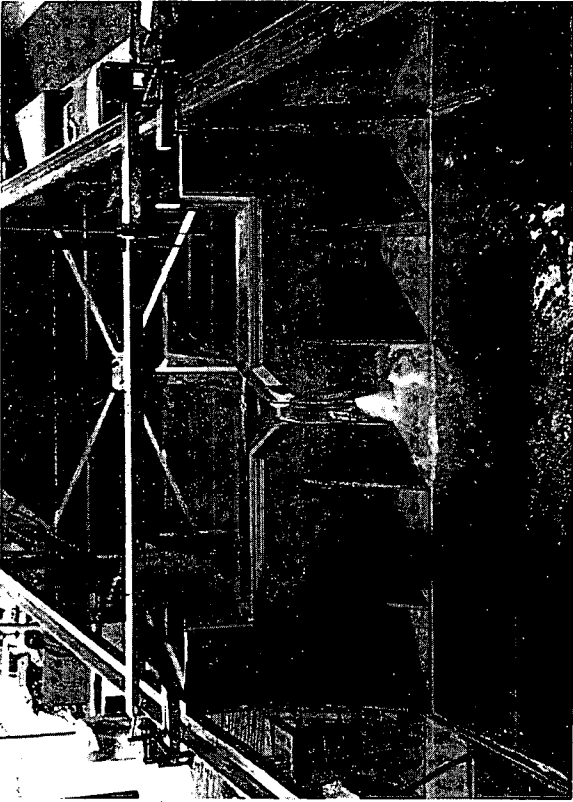
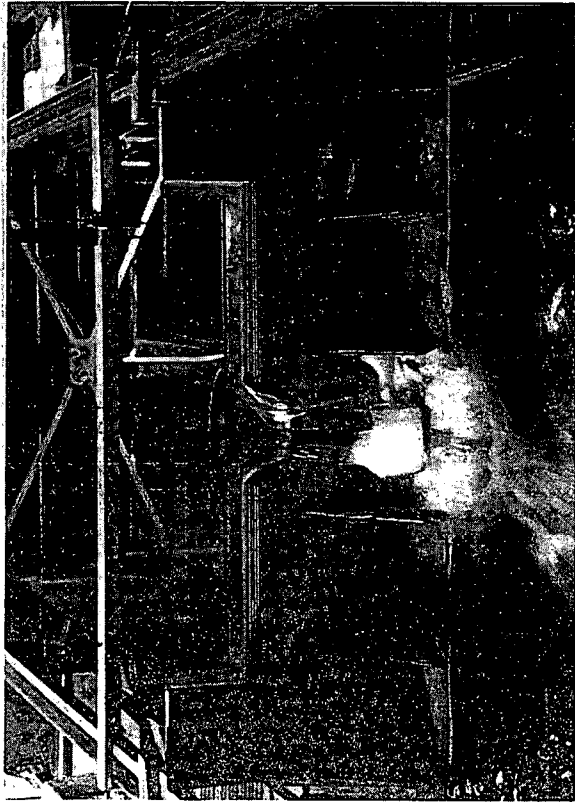


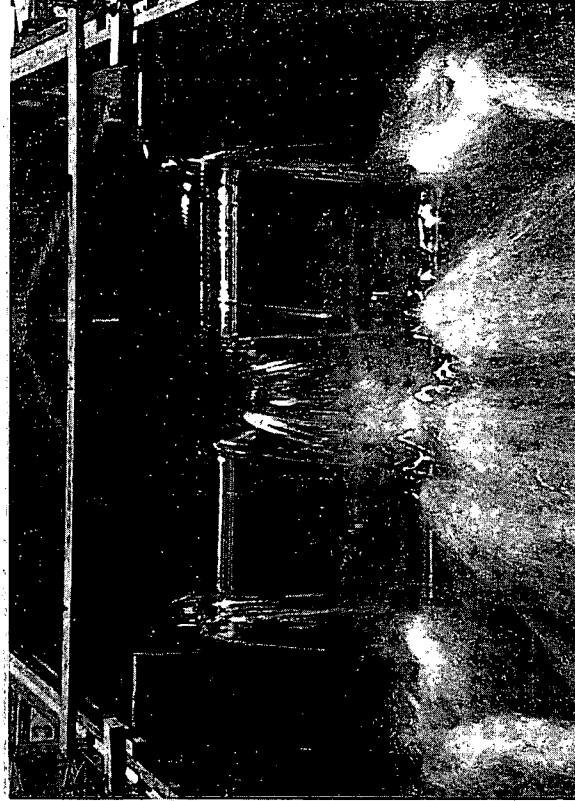
Figure 9. STILLING WELLS FOR WEIR MODEL



H = 7.30 cm



H = 15.01 cm



H = 29.95 cm

FIGURE 12. COMPOUND WEIR AT LOW, MEDIUM AND HIGH FLOWS

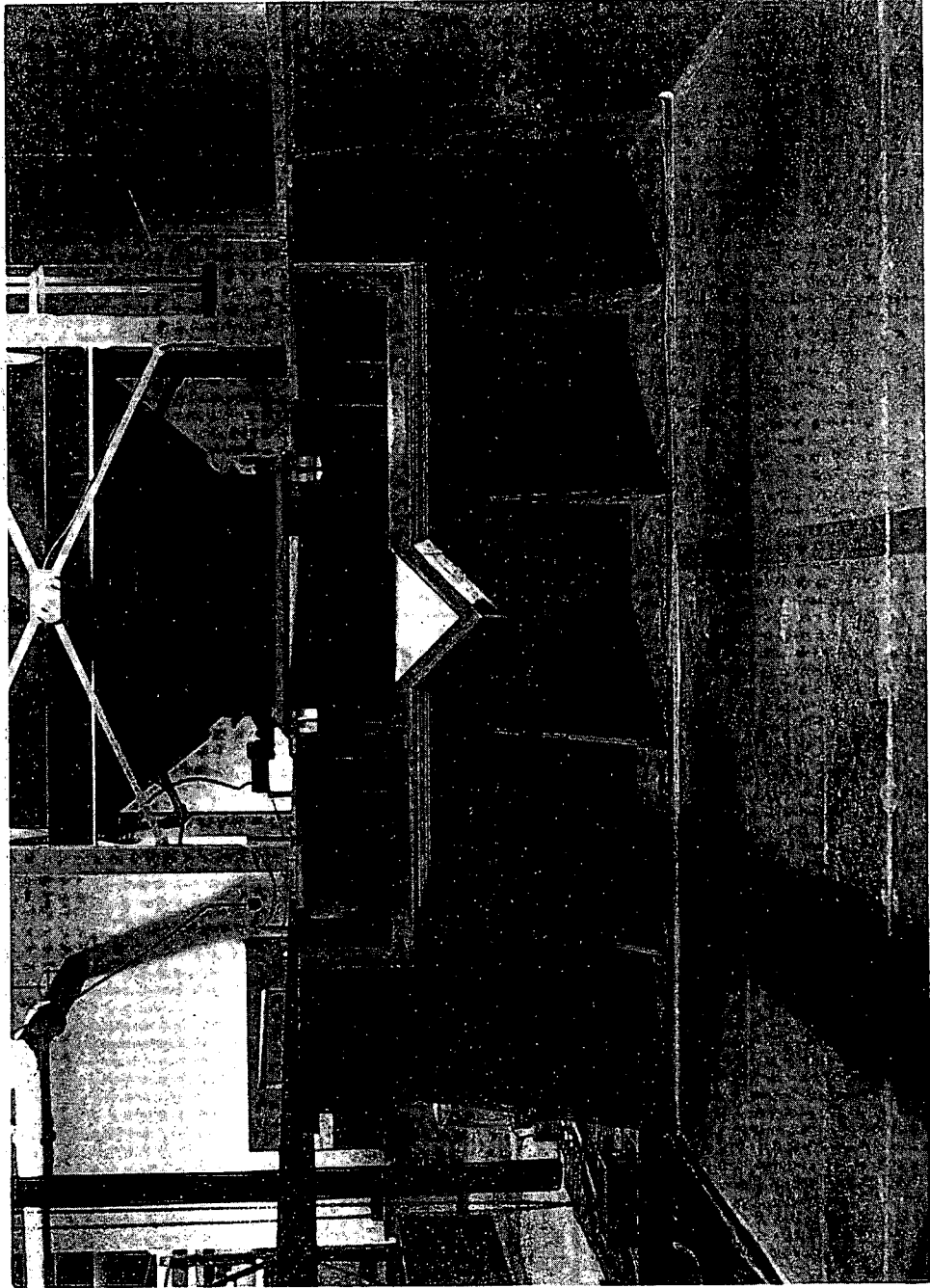


FIGURE 10. COMPOUND WEIR IN FLUME

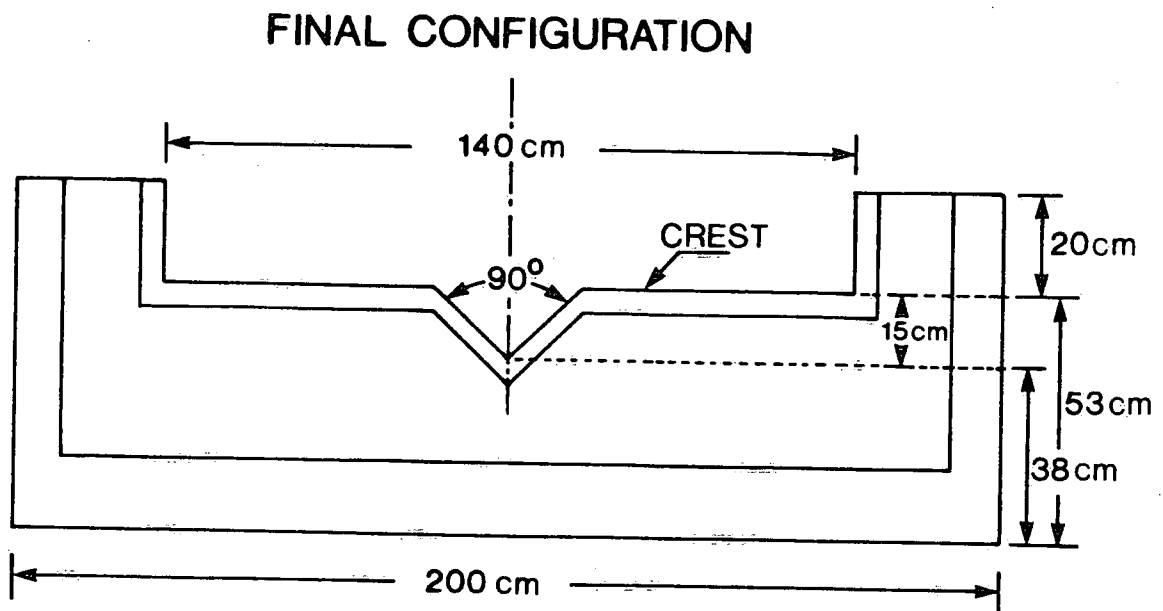


FIGURE 11. DIMENSIONS OF COMPOUND WEIR

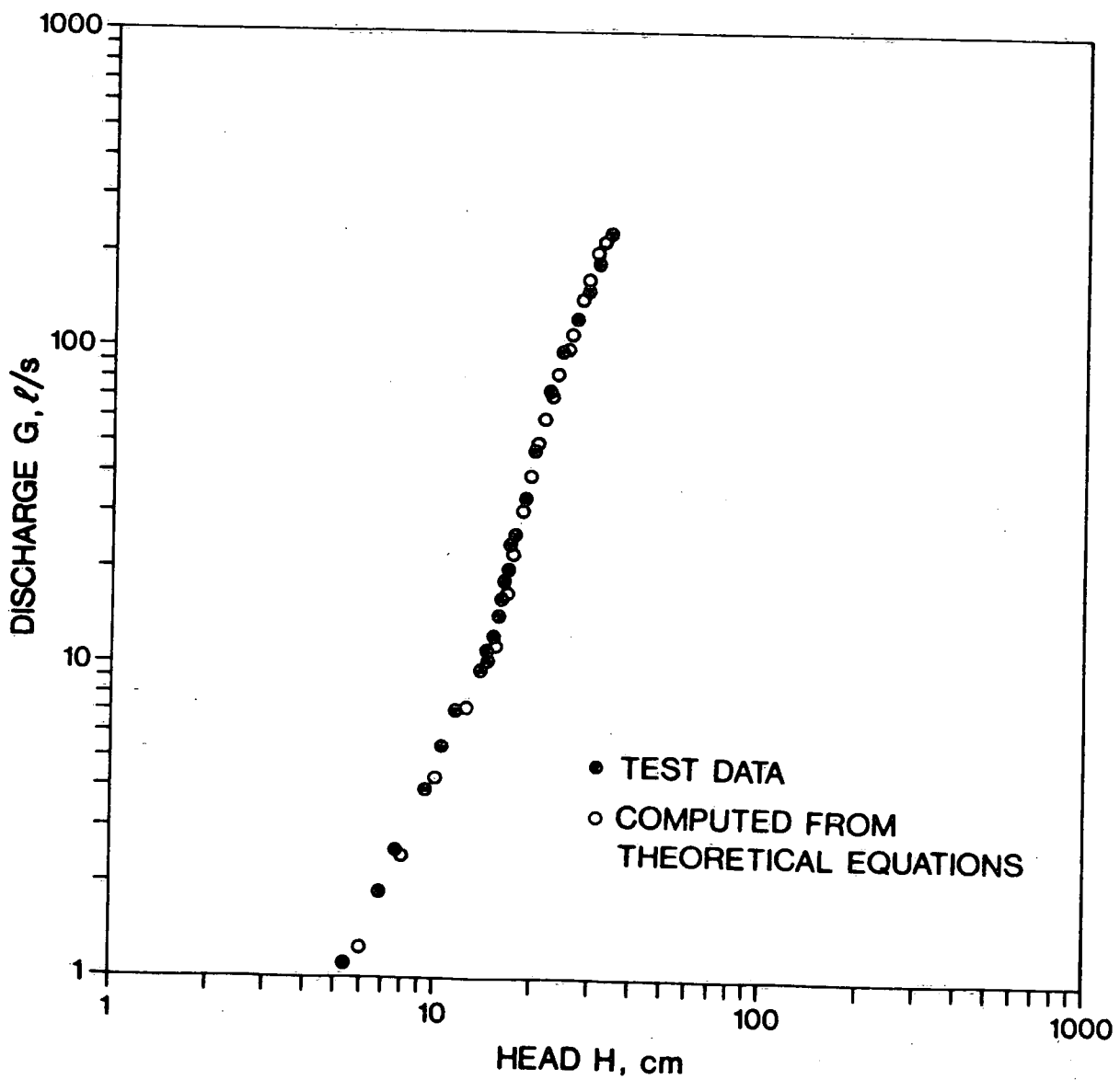


FIGURE 13 PLOT OF TEST RESULTS AND THEORETICAL EQUATIONS

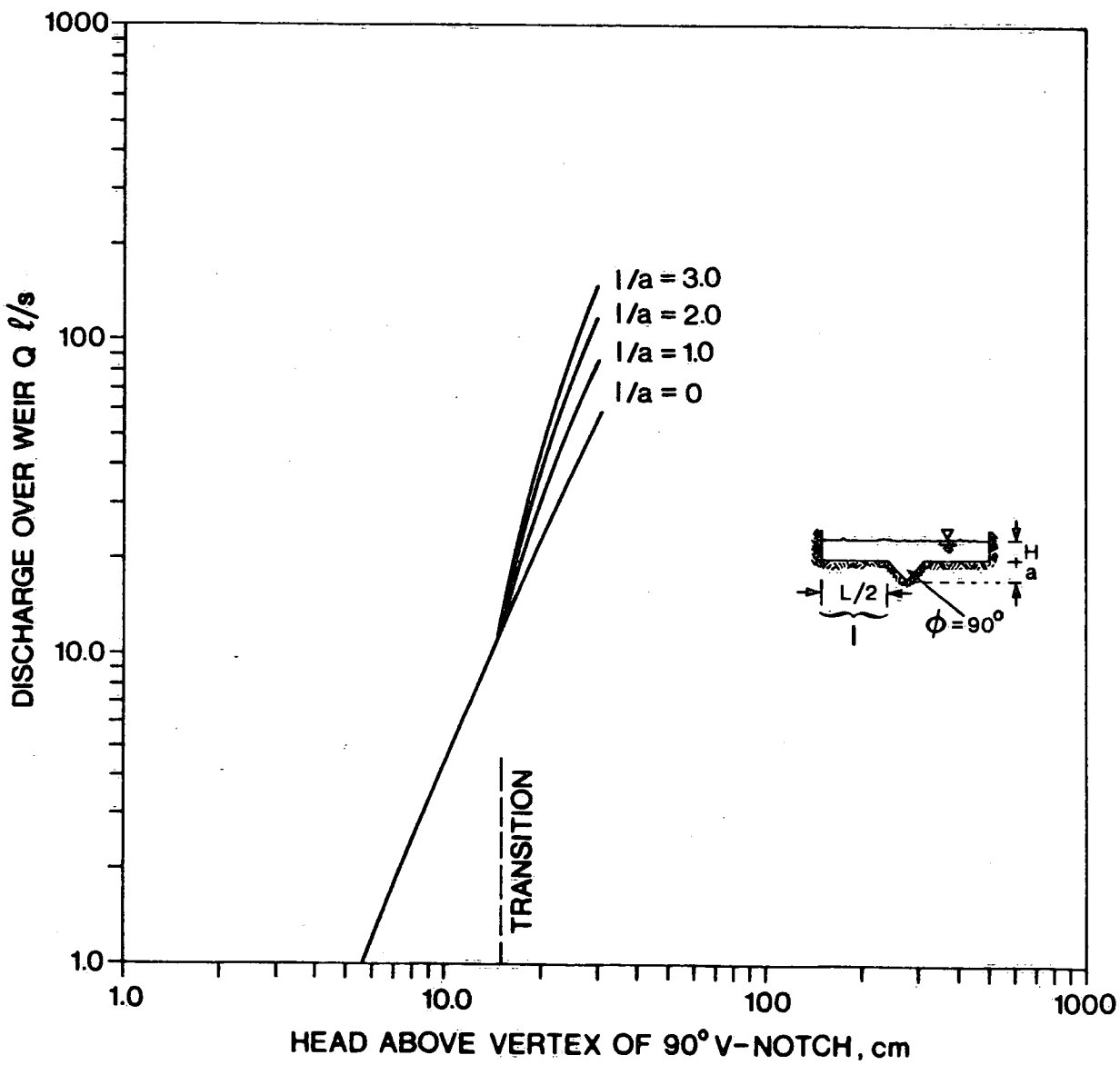


FIGURE 14. EFFECT OF l/a ON STAGE-DISCHARGE CURVE